# CORRELATION OF PERFORMANCE DATA FOR ELECTRIC SUBMERSIBLE PUMPS WITH GAS-LIQUID FLOW

J. F. Lea, Amoco Production Company
J. L. Turpin, University of Arkansas
J. L. Bearden, Centrilift Hughes, Inc.

## INTRODUCTION

It is known that the presence of free gas in a liquid affects the performance of a centrifugal pump. Test work as early as 1929 was concerned with the possibility of controlling pump output and, thus, conserving power by admission of air to the pump suction ([1] as reviewed in [2]), although this idea has long since been abandoned [3]. Published studies of the effects of entrained air on the performance of a submersible centrifugal pump are presented in References [4], [5].

This paper describes a program to define the effects of free gas on the performance of electric submersible centrifugal pumps. The effects of the free gas show up as a deterioration of the head-capacity curve, such as areas of unstable head production, and effects similar to cavitation at higher flow rates. Depending on the amount of free gas through the pump, these effects may vary from slight interference to gas locking.

Gas interference is indicated on the surface amp chart by rapid variation of the motor loading. Gas locking occurs when the pump ingests too much gas and actually stops pumping because its head (or pressure) production is drastically decreased. This causes the motor to unload and to shut down because of low ampere surface control protection.

When designing an electric submersible pump for a gassy application, it is desirable to know the amount of free gas the pump can tolerate and to compare this to downhole gas conditions. Thus, the objectives of this project were (1) to generate experimental data relating pump performance (i.e., head-capacity) to gas-liquid ratio at the pump suction and to the pump suction pressure, (2) to correlate these data, and (3) to develop a model which would predict head-capacity performance of a submersible pump as a function of gas-liquid ratio, suction pressure, pump type, and any other pertinent parameter.

---

These results previously presented at the Texas A&M Symposium on centrifugal pumps (1986).

Experimental data examined here were collected by two independent research efforts, as described in reference [5]. Tests conducted by Amoco Production Research Company involved using water and air. A separate program was conducted for Centrilift Hughes, Inc. at the R. C. Ingersoll Research Center using diesel fuel and $CO_2$. In both programs, the purpose of the tests was to define the performance of typical submersible centrifugal pump stages when free gas volumes were introduced at the pump suction under various flow and pressure conditions.

The two test facilities and programs are described in reference [5], and results from each are presented and discussed.

## FACILITIES AND PROCEDURES FOR AIR/WATER TESTS

The test facility at Amoco was an above-ground installation in which the flow patterns and distribution of air volumes could be viewed. For simplicity, water and air were chosen as working fluids. A schematic of the test loop is shown in Figure 1. The pump housing, containing five Centrilift I-42 pump stages, was installed in an 8-in.-OD, 7-in.-ID plexiglas tube. Because of the plastic container, the annulus backpressure was restricted to low pressures, with the majority of the tests being run at 25-30 psig.

The system was designed so that the water flows through the system in a closed loop, but the air was directed to make a single pass through the pump or annulus before separation and venting. The injected air that did not enter the pump continued up the annulus and out through a backpressure regulator. The air entrained into the pump was separated from the fluid stream in a gas separator downstream of the pump and was vented through floating ball rotometers for measurement. See reference [5] for additional details.

## DATA REDUCTION AND RESULTS FOR AIR/WATER TESTS

The data collected were reduced in a form to compare with published performance curves, including the head, efficiency, and horsepower performance values.

The motor horsepower delivered to the system was calculated. To obtain this value, the amperage through each of the three motor leads was measured at 400 V supply and used to calculate the motor horsepower published curves.

The average head, h, produced for one stage was calculated from the measured delta pressure across the pump and a calculated bulk density for the air/water mixture based on the following expression:

$$h = \frac{\Delta p(144)}{F_{wv\ aw}(n)} \tag{1}$$

where: $\Delta p$ = delta pressure across the pump, psi

$n$ = number of stages

$F_{wv\ aw}$ = average weight density of the air/water mixture through the pump, lbf/ft$^3$,

and

$$F_{wv\ aw} = \frac{F_{wv\ w} \times q_w + F_{wv\ a} \times q_a}{(q_w + q_a)} \tag{2}$$

where: $F_{wv\ w}$ = weight density of water, lbf/ft$^3$,

$F_{wv\ a}$ = weight density of air, lbf/ft$^3$, at the average pressure between stage inlet and outlet pressure, lbf/ft$^3$,

$q_w$ = volumetric flow rate of water, gal/min, and

$q_a$ = volumetric flow rate of air at the average pressure between stage inlet and outlet pressure, gal/min

The efficiency, E, of the pump for one stage was found from the ratio of the output hydraulic horsepower to the input horsepower as calculated from amperage and voltage data and the motor curves:

$$E = \frac{\Delta p(144)(q_w + q_a)}{(hp)(7.48)(60)(550)(n)} \tag{3}$$

where hp is horsepower.

## Results

The results (data points) for head only are shown versus published performance curves (smooth line) on Figure 2, repeated here from reference [5]. The data collected were focused on the recommended operating range. Each data set shows a different value of percent by volume of gas at pump intake. The results show the beginning of serious departure from the head curves at about 7% free gas by total volume and intermittent gas locking at about 11%. The bands of calculated head shown when surging begins indicate the head oscillated from high to low values with a frequency of a second or two. Although there is still the periodic head produced for still greater than 11 vol% of gas at pump intake, the pump is not performing near published head values once the percent by volume of gas exceeds some point between 7 and 11 vol% by intake. These tests all were made at 25-30 psig pump intake pressure.

## FACILITIES AND PROCEDURES FOR DIESEL/$CO_2$ TESTS

A simple closed-loop system was designed to test various submersible pumps. Simplicity was desirable because of the problems encountered with two-component flow.

A schematic of the test facility is shown in Figure 3. The casing (1), which housed the submersible pump (2), is 8-in. pipe, and the flowline (3) is made up of 2-in. pipe. The casing was designed so that various flow inlets (4 and 4a) could be used, and two windows (5) were mounted so that flow at the pump inlets could be observed. A sheet metal baffle (6) was placed between the casing and pump. The baffle has the same inside dimensions as a 7-in. casing and forces the fluid to follow a path similar to an actual deep well setting. The pump was belt-driven by a 7-1/2 hp vertical surface motor (7) mounted below the casing base flange. The non-electrical instrumentation consisted of a positive displacement flowmeter (8), a differential pressure gauge (9) between the pump intake and discharge, a pressure gauge (10) for casing static pressure, and temperature thermocouples and gauges.

The test fluids were diesel fuel and $CO_2$. These fluids were chosen to test with a gas solubility effect present similar to actual oilwell production fluids. See reference [5] for additional discussion.

## Test Program

For each test, the loop was filled with diesel, and then a percentage of the total enclosed volume was displaced with $CO_2$. After the desired amount of diesel was displaced for a particular test, the pump was started and the static system pressure was stabilized with an additional amount of $CO_2$. Once the system was stabilized at the desired test loop pressure and liquid volumetric percentage, the pump performance tests were started.

Numerous tests were conducted on several different types of pump stages: a radial pump stage designed for 42-gal/min optimal flow (Centrilift Hughes, I-42B), a radial pump stage with an optimal flow rate of 73 gal/min (C-72), and a mixed flow pump stage with an optimal flow rate of 80 gal/min (K-70) (Fig. 4). The last two stages provided a comparison of two different design styles with the same approximate design flow rate.

## DATA REDUCTION AND RESULTS FOR DIESEL/$CO_2$ TESTS

The data collected for the various fluid mixture and pressure tests were plotted as pressure/flow rate curves and compared against the pump's pressure/flow rate performance with 100% diesel.

The tests (Figs. 5-7) run on the I-42B pump were reduced from pressure to feet of head so they could be compared with the air/water tests run on the same type stages. The pressure was reduced to head by using an equation similar to Eq. (1). The average fluid gravity, Eq. (2), was modified to account for the diesel/$CO_2$ volume factor (2%/100 psig).

### Results

The results of the diesel/$CO_2$ tests are shown in Figures 5-11. The first three curves are for an eight-stage I-42B pump, the same type as used in the air/water tests. Figures 5, 6, and 7 show the results of varying liquid/gas volumes at 50-, 100-, and 400-psig pump intake pressures. Several conclusions can be reached from these three curves. First, pump performance is a function of both the percent of free gas by volume and pump intake pressure. In general, the head measured to the right of the performance curves drops as intake pressure decreases. The higher intake pressures require lower percent gas compression through the pump. Second, at rates equal to or greater than 15 vol% gas, the pump enters an area of severe head oscillation at flow rates less than the volume flow at the design point, which in this case was about 50 gal/min. And finally, at higher flow rates, the head takes a nearly vertical dip, which is similar to the effect of cavitation. It is noticed that the calculated head values for the lowest gas volume present (10%) at 50 and 100 psig are above the diesel-only base curves. This may be explained as caused by gas holdup in the system, where a small percentage of gas holdup is a large percentage of the total gas in the system. Therefore, fluid through the pump can be approaching a pure liquid and perhaps should not be corrected uniformly to account for gas presence as was done here. Also, although the gas presence decreases pressure output, the use of mixed density equations may simply not be adequate to describe head production over some ranges of performance.

The effects of gas on the performance of different types of stages (mixed and radial) are shown in Figures 8-11. The mixed-flow design, K-70, is represented in Figures 8 and 9, and the radial design, C-72, is shown in Figures 10 and 11. Both stages are designed for the same approximate design flow rate. Therefore, any difference in the ability to handle gas would be attributed to their design differences. From the test results, note that even though both stages have a surging region, the mixed-flow design has less deterioration in its pressure/flow rate curve. Therefore, as a pump stage tends toward a highly mixed or axial flow design, its gas-handling capability should increase. Even though the K-70 pump had less deterioration in head than the C-72 pump, both types entered a pressure oscillation or surging area at flow rates at or less than the optimal design flow rate.

## CORRELATION OF THE DATA

Eighty-six experimental head-capacity curves were utilized to develop the correlations. There were 12 sets of data for the I-42 pump operating on air-water, 24 sets of data for the I-42 with $CO_2$-diesel, 24 sets of data for the C-72 with $CO_2$-diesel, and 26 sets of data for the K-70 pump with $CO_2$-diesel.

For a given pump, the controlling factors used to describe the deterioration of head were the gas-liquid ratio, the suction pressure, and the capacity. That is,

$$\frac{H}{H_{sp}} = \psi \left[\frac{q_s}{Q}, P_s, Q\right] \qquad (4)$$

where: $H$ = head with gas-liquid flow

$H_{sp}$ = head with single-phase liquid flow

$\psi$ = indicates a function of following quantities

$q_s$ = volumetric flow rate of gas at pump suction,

$Q$ = volumetric flow rate of liquid at pump suction,

$P_s$ = pressure at pump suction, and

Establishing the functional form of Eq. (4) required considerable trial and error. Crossplots indicated a general exponential decay in performance with $q_s/Q$. The resulting correlations for each of the three pumps are included in the Appendix. The correlations predict the head-capacity curve fairly well for low gas at low suction pressures and for higher gas volumes at higher suction pressures. The prediction falls off in the direction of higher gas and lower pressure conditions. However, the region of poor predictive capability of the correlations coincides with the region of unacceptable pump performance. The correlations only hold in general to the right of the best efficiency point and, as the data shows, stable head production with gas only occurs in this region as the gas percentage increases.

A second relationship was developed to quantify the region of unacceptable pump performance. This was done by noting the pump performance at the various combinations of gas-liquid ratio and suction pressure employed. A quantity $\phi$ was defined as:

$$\phi = \frac{2000\ (q_s/Q)}{3\ P_s} \tag{5}$$

with $P_s$ in units of psia. Plots of data with various $\phi$ values are shown in Figures 12-14 against the correlations shown in the Appendix. Note that, in general, if the $\phi \leq 1.0$, then the correlations are fairly accurate, and, of perhaps more importance, the head produced is still a substantial fraction of liquid only head. Values other than 1 could be chosen to be more or less conservative.

The following example illustrates how $\phi$ could be used to predict whether or not a gassy well could be pumped with a downhole centrifugal pump or not.

<u>Example</u>

Given the following data:

WOR (water to oil ratio) = 1.0

calculate the gas volume $q_s$ (in bbl/d) at $p_s$:

$$q_s = Q_o(\mathrm{GOR}-R_s)\cdot\frac{14.7}{p_s}\cdot\frac{T+460}{520}\cdot z\cdot\frac{1}{C} \tag{6}$$

where: $Q_o$ = oil flow rate, bbl/d

$R_s$ = solution GOR, SCF/bbl

$T$ = pump intake temperature, $^{o}F$

$C = 5.61\ ft^3/bbl$ (conversion factor)

Calculate the liquid volume at pump suction in bbl/d:

$$Q = Q_o\ (WOR + B_o) \tag{7}$$

where: $Q$ = total liquid volume rate at $p_s$, bbl/d

$B_o$ = formation volume factor (oil swellage factor), bbl/bbl

Using Standing's correlations for $R_s$ and $B_o$ (see reference [6]), the following procedure can be used to calculate $p_s$ (minimum) from $\phi = (2000(q_s/Q))/3\ p_s$ where $\phi = 1.0$.

<u>Procedure</u>

1. Guess $p_s$.
2. Calculate $q_s$, Q, $P_s$ given the $\phi$ relationship and above expressions.
3. Compare $p_s$ to guessed $P_s$.
4. Return to step 1. until old ≅ new $P_s$ calculated.

Once $p_s$ is found as a function of GOR, it can also be calculated as a function of % gas at suction:

$$\%\ gas = \frac{q_s}{q_s + Q} \times 100 \tag{8}$$

Figure 15 shows intake pressure as a function of % gas at the intake and also versus various possible well GOR's.

In Figure 16, a family of hypothetical IPR (Inflow Performance Relationships) for a well are plotted. A straight line relationship is calculated above a calculated bubble point. The IPR's are constructed with the shut-in well pressure = 3000 psi and a test point of 300 bbl/d at 1500 psi bottomhole pressure. Vogel's IPR curve (reference [7]) is used to complete the curves below the bubble point. Note the five IPR's are shown with GOR's ranging from 0 to 400 SCF/bbl. Disregarding NPSH requirements, the 0 GOR well could be pumped off. However, as the GOR reaches 400, the well cannot be pumped off below $P_s$ = 520 psi without the $\phi$ correlation indicating the pump would not perform satisfactorily with free gas present.

This correlation allows a potential pump user to predict when gas becomes a problem. Then a gas separator can be used or less drawdown of the well can be expected. Some additional stages should be added to account for head deterioration with gas. The additional stages required could be estimated from the correlations in the appendix or from examination of test data presented. The pump should be designed to operate to the right of the head curve to avoid surging when gas is expected through the pump.

## CONCLUSIONS

An empirical model was developed to predict the head-capacity curve for electric submersible centrifugal pumps as a function of gas-liquid ratio and suction pressure. Approximate correlations for the I-42, the C-72, and the K-70 pump are given by Eqs. (A-1) to (A-5) of the Appendix. The correlations show exponential decay of head with increasing $(q_s/Q)$.

The regions of reasonably good pump performance coincide with the regions of applicability of the correlations. These regions are identified by a parameter, $\phi$, defined as:

$$\phi = \frac{2000\ (q_s/Q)}{3\ P_s} \tag{9}$$

$\phi \lesssim 1$, correlations applicable and good head production with gas present

$\phi \gtrsim 1$, correlations not applicable, but pump performance is in general so poor that operation in these regions is to be avoided.

Representative values from Eq. (9) indicate that each of the pump stages tested will tolerate about 13% gas (by volume) at 100 psia suction pressure and up to 37% gas at 400 psia suction pressure with no serious deterioration of head performance. Test results show stable head production only at rates higher than the design point as the gas volume at suction increases until more gas finally completely gas locks the pump.

## REFERENCES


1. Seibrecht, W., "Untersuchungen uber Regelung von Kreiselumpen," Z. Ver. Deut. Ing., 74, 87, 1930.

2. Stepanoff, A., Centrifugal and Axial Flow Pump, 2nd edition, 230, Wiley & Sons, 1957.

3. Stepanoff, A., Pumps and Blowers - Two-Phase Flow, 264, Krieger Publishing Company, 1978.

4. Murakami, M. and Minemura, K., "Effects of Entrained Air on the Performance of a Centrifugal Pump," JSME, 17, 110, 1047-1055, and 17, 112, 1287-1295, Oct. 1974.

5. Lea, J. F. and Bearden, J. L., "Effect of Gaseous Fluids on Submersible Pump Performance," JPT, 2922-2930, Dec. 1982.

6. Frick, Thomas C., "Petroleum Production Handbook," II, New York, McGraw-Hill Book Co., 1962.

7. Vogel, J. V., "Inflow Performance Relationship for Solution Gas Drive Wells," JPT, 83-93, Jan. 1968.

## APPENDIX A

Approximate correlation of the data for the I-42 and the K-70 pumps is achieved by:

$$\frac{H}{H_{sp}} = e^{-a(q_s/Q)} \tag{A-0}$$

with "a" given by:

$$a = \frac{346430}{P_s^2}\left(\frac{q_s}{Q}\right) - \frac{410}{P_s} \tag{A-1}$$

Correlation of the data for the C-72 pump is by:

$$\frac{H}{H_{sp}} = e^{-a(q_s/Q)}\,[1 - 0.0258\,(Q-Q_D)$$

$$+ 0.00275\,(Q-Q_D)^2 - 0.0001\,(Q-Q_D)^3 \tag{A-2}$$

with

$$Q_D = 98.3 - 33.3\,\phi \tag{A-3}$$

and

$$a = \frac{285340}{P_a^2}\left(\frac{q_s}{Q}\right) \tag{A-4}$$

The correlations are designed for flow higher than that of the best efficiency point. They lose accuracy rapidly as $\phi$ begins to exceed 1, but the exponential drop in head with increasing $q_s/Q$ is a general characteristic.

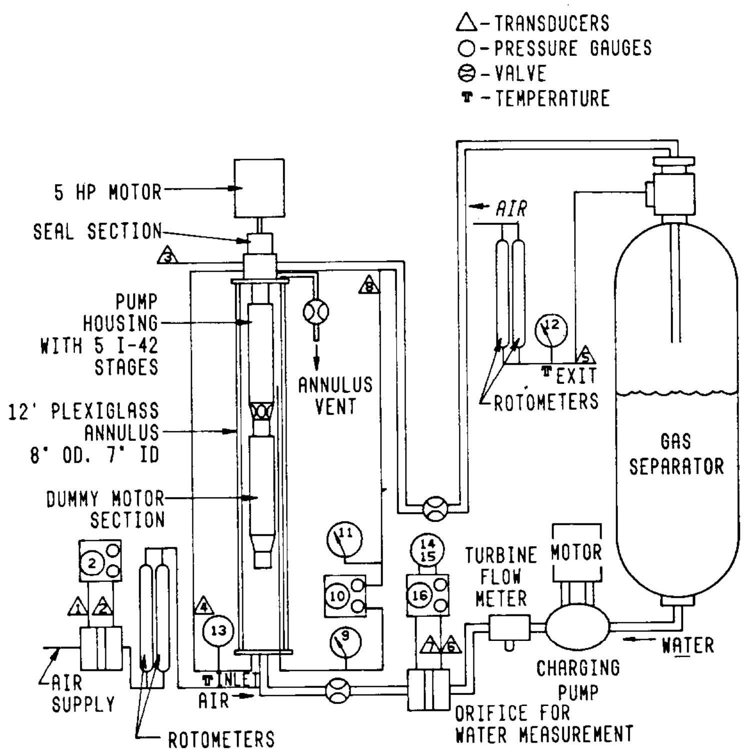


Figure 1 - Schematic of test facility

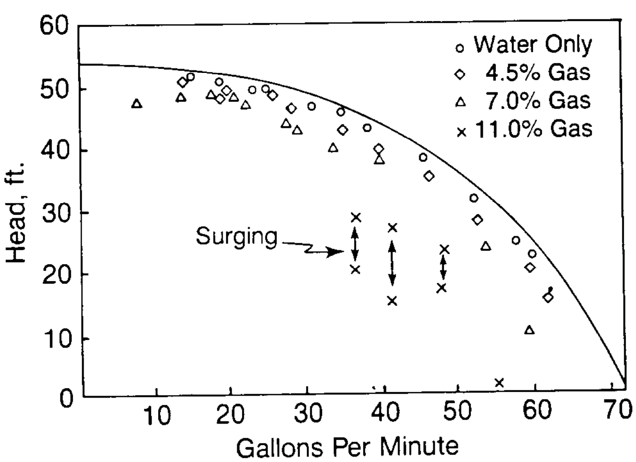


Figure 2 - Deterioration of water head curves with gas (Ref 5)

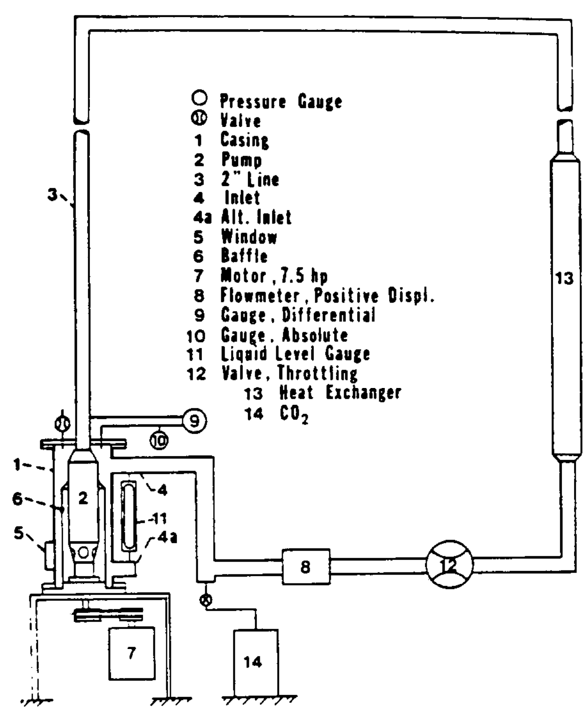


Figure 3 - Research pump test facility

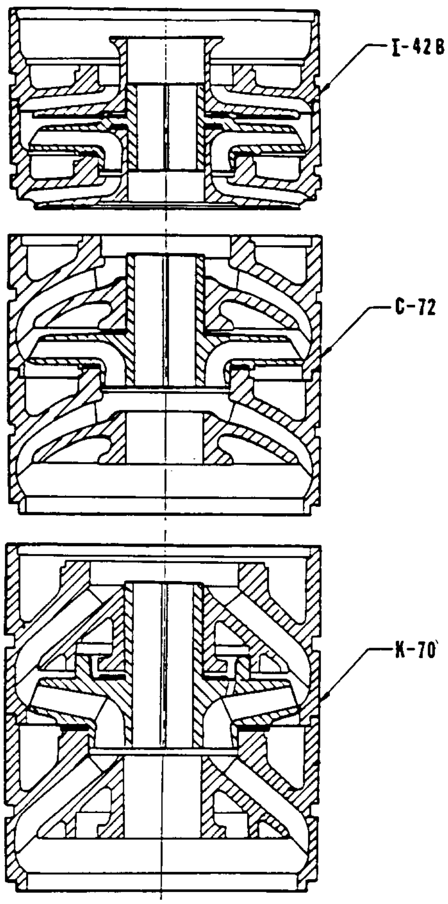


Figure 4 - Pump stages tested

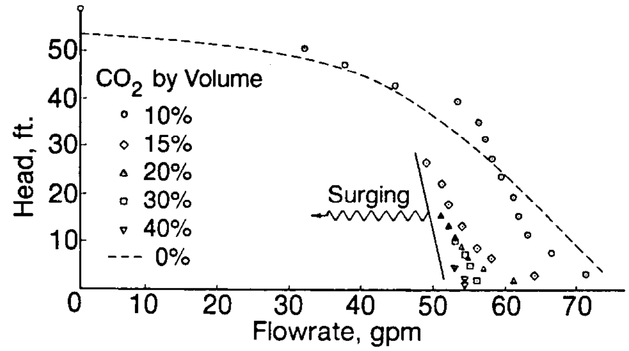


Figure 5 - Diesel/$CO_2$, 50-psig intake pressure, I - 42B pump

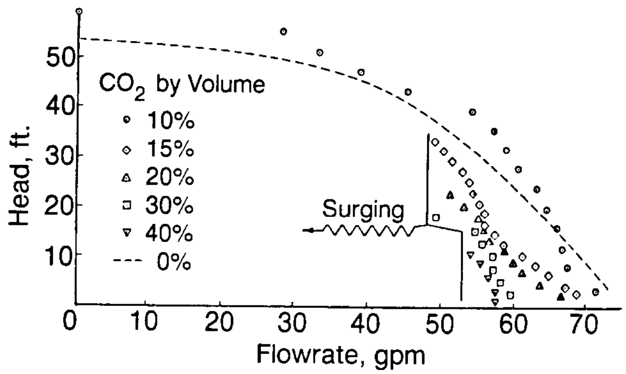


Figure 6 - Diesel/$CO_2$, 100-psig intake pressure, I - 42B pump

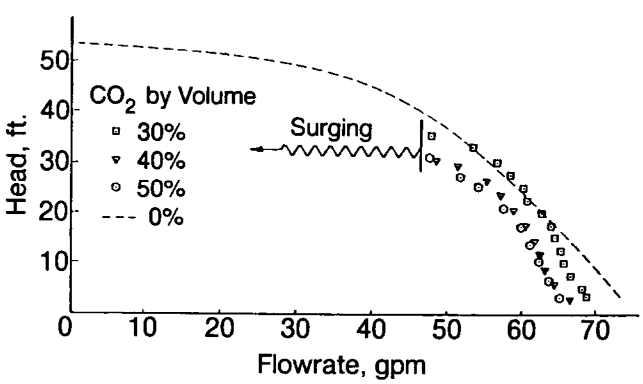


Figure 7 - Diesel/$CO_2$, 400-psig intake pressure, I - 42B pump

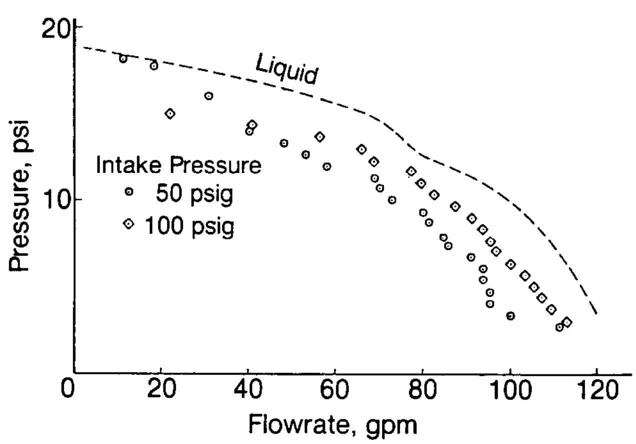


Figure 8 - Diesel/$CO_2$, 10 vol% $CO_2$, K-70 pump

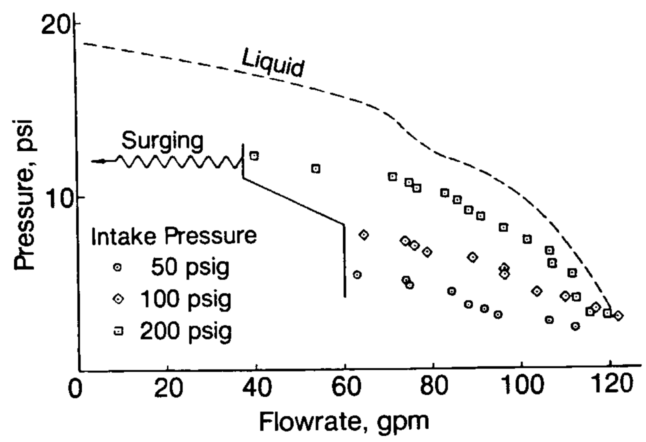


Figure 9 - Diesel/$CO_2$, 15 vol% $CO_2$, K-70 pump

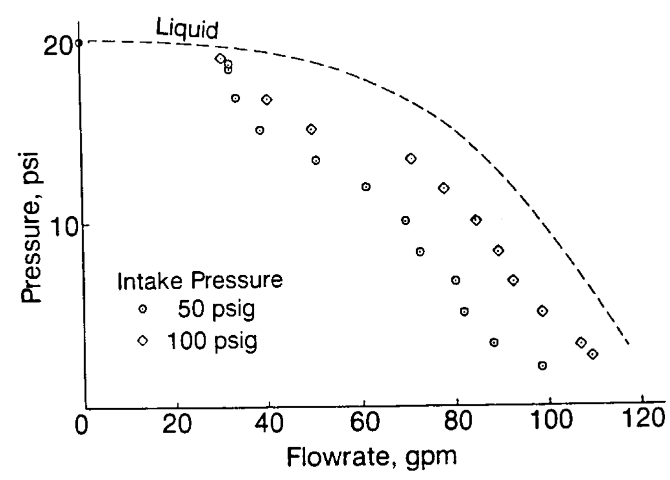


Figure 10 - Diesel/$CO_2$, 10 vol% $CO_2$, C-72 pump

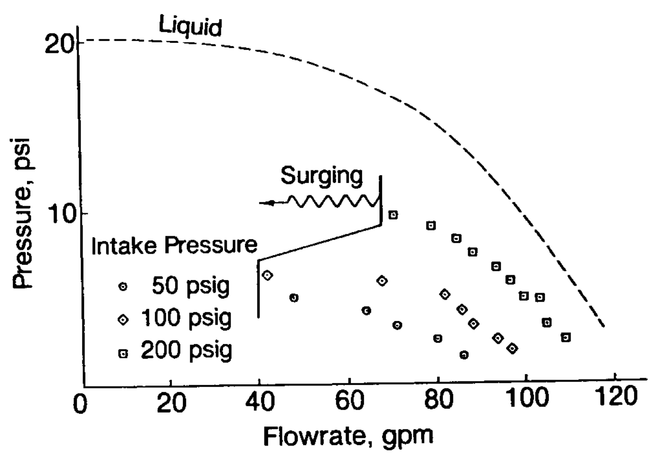


Figure 11 - Diesel/$CO_2$, 15 vol% $CO_2$, C-72 pump

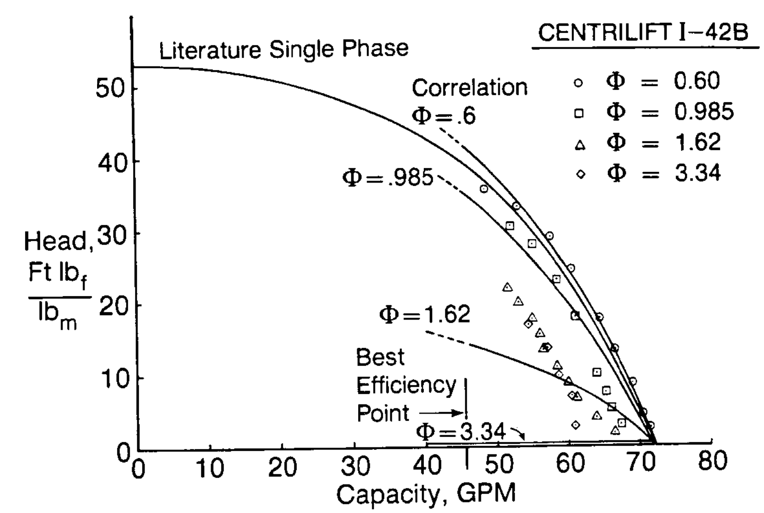


Figure 12 - Pump performance deterioration for I-42

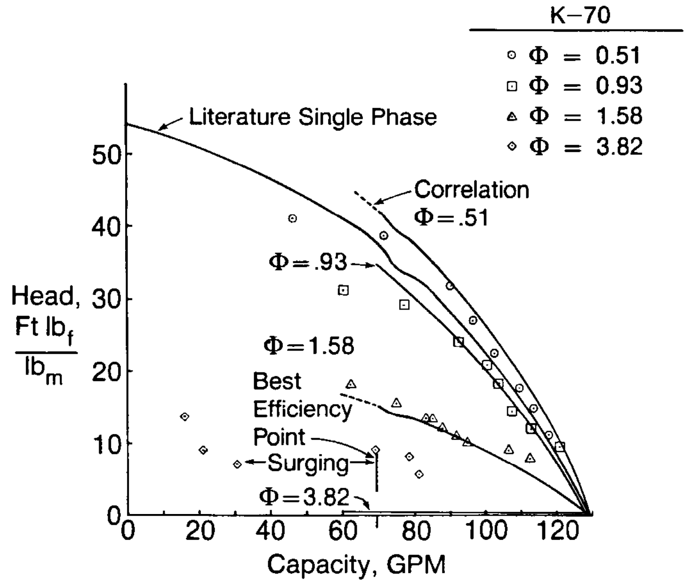


Figure 13 - Pump performance deterioration for K-70

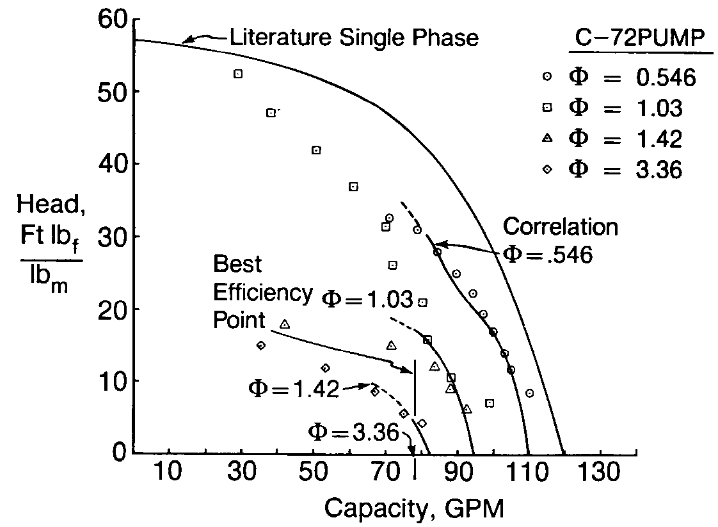


Figure 14 - Pump performance deterioration for C-72

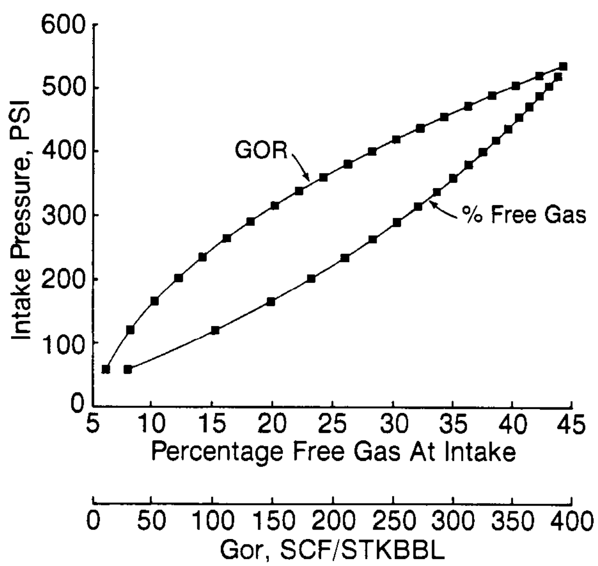


Figure 15 - Acceptable free gas correlation for ESPS

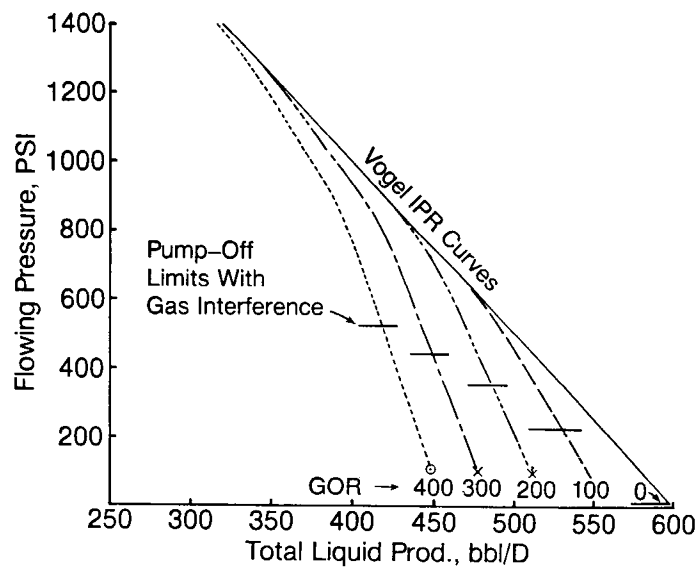


Figure 16 - Example of pump - off limits for reservoirs with various GOR's